DALTON

Synthesis, spectroscopic characterisation, electron-transfer properties and crystal structure of $[Ru^{II}(bipy)_2(2\text{-}SC_5H_4N)]ClO_4$ (bipy = 2,2′-bipyridine)

Bidyut Kumar Santra,[a] Mahua Menon,[b] Chandan Kumar Pal[b] and Goutam Kumar Lahiri*[,a]

[a] *Department of Chemistry, Indian Institute of Technology, Powai, Bombay-400076, India*
[b] *Department of Inorganic Chemistry, Indian Association for the Cultivation of Science, Calcutta-700032, India*

Two new ruthenium(II) mixed-ligand tris-chelated complexes of the type $[Ru(bipy)_2L]ClO_4$, (bipy = 2,2′-bipyridine; L = pyridine-2-thiolate **1** or pyridin-2-olate **2**) have been synthesized. The complexes are essentially diamagnetic and behave as 1:1 electrolytes in acetonitrile solution. They display two metal-to-ligand charge-transfer (m.l.c.t.) transitions near 500 and 340 nm respectively along with intraligand transitions in the UV region. Both exhibit room-temperature emission from the highest-energy (m.l.c.t.) band. At room temperature the lifetime of the excited states for the thiolato (**1**) and phenolato (**2**) complexes are 100 and 90 ns respectively. The geometry of the complexes in solution has been assessed by high-resolution ^{1}H NMR spectroscopy. The molecular structure of complex **1** in the solid state has been determined by single-crystal X-ray diffraction. It shows the expected pseudo-octahedral geometry with considerable strain due to the presence of the sterically hindered ligand L^1. In acetonitrile solution the complexes show quasi-reversible ruthenium(II)–ruthenium(III) oxidation couples at 0.54 and 0.64 V *versus* saturated calomel electrode and quasi-reversible ruthenium(III)–ruthenium(IV) oxidations at 1.41 and 1.03 V respectively. Two reversible reductions are observed near −1.6 and −1.9 V for each complex due to electron transfer to the co-ordinated bipy units. The trivalent analogues of **1** and **2** are unstable at room temperature but can be generated in solution by coulometric oxidation at 263 K as evidenced by EPR spectroscopy.

Since the discovery of important redox, photophysical and photochemical properties of ruthenium complexes having 2,2′-bipyridine (bipy) as ligand, there has been continuous research activity in the direction of developing newer ruthenium–bipyridine systems with the perspective of interesting physicochemical properties. In this context different kinds of mixed-ligand ruthenium–bipyridine complexes have been synthesized and studied over the last fifteen years.[1] The basic strategies behind all these activities are either to incorporate different groups within the bipyridine moiety itself or use other types of donor sites along with the $Ru(bipy)_2$ core to form mixed-ligand tris-chelates to modulate the photoredox activities of this class of complexes.[2] The present work originates from our interest in preparing new mixed-ligand ruthenium–bipyridine complexes of type $[Ru(bipy)_2L]$, where L is a ligand which can form a four-membered chelate ring on co-ordination and in studying the effect of the sterically hindered L on the redox and spectroscopic properties of the $Ru(bipy)_2$ core. As part of our programme we have chosen pyridine-2-thiol and pyridin-2-ol as ligand L. Herein we report the synthesis of two complexes having RuN_5S and RuN_5O chromophores, their spectroscopic characterisation, electron-transfer properties, spectroelectrochemical correlation, preliminary photophysical aspects, crystal structure of the thiolato derivative and electronic structures of the electrogenerated trivalent congeners. To our knowledge this work demonstrates the first example of $[Ru(bipy)_2L]$ systems where L is a sterically hindered four-membered pyridine-derived ligand.

Results and Discussion

Synthesis

The two ligands pyridine-2-thiol and pyridin-2-ol are abbreviated as HL^1 and HL^2 respectively. The anionic forms of the ligands (L) bind to the metal ion in a bidentate N,S and N,O manner respectively forming four-membered chelate rings.

$$[Ru(bipy)_2Cl_2]\cdot 2H_2O \xrightarrow{(i)} [Ru(bipy)_2(EtOH)_2]^{2+}$$
$$\downarrow (ii)$$
$$[Ru(bipy)_2L^1]^+ \quad \mathbf{1}$$

Scheme 1 (*i*) $AgClO_4$, EtOH, heat; (*ii*) HL^1, NaO_2CMe, N_2, heat

$$[Ru(bipy)_2(CO_3)] + HL^2 \xrightarrow{(i)} [Ru(bipy)_2L^2]^+ + HCO_3^- \quad \mathbf{2}$$

Scheme 2 (*i*) EtOH, NaO_2CMe, heat, stirring

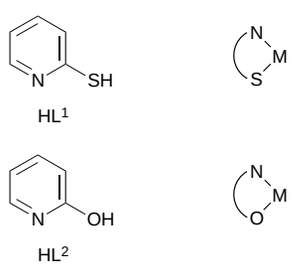

The complex $[Ru(bipy)_2L^1]^+$ **1** has been synthesized from $[Ru(bipy)_2Cl_2]\cdot 2H_2O$ following the synthetic route shown in Scheme 1. The complex cation was precipitated directly from the reaction mixture as its perchlorate salt. The crude product was purified by column chromatography using a silica gel column. The route used to prepare $[Ru(bipy)_2L^2]^+$ **2** was different, involving an ethanolic solution of $[Ru(bipy)_2(CO_3)]$ and HL^2 with heating and stirring in the presence of NaO_2CMe (Scheme 2). The cationic complex **2** was isolated pure as its perchlorate salt. The yield of the complexes was approximately

Table 1 Microanalytical,[a] conductivity[b] and electronic spectral data[c]

Compound	Analysis (%) C	H	N	Λ_M/Ω^{-1} cm^2 mol^{-1}	UV/VIS λ/nm (ε/dm^3 mol^{-1} cm^{-1})
1	48.1 (48.15)	3.1 (3.2)	11.15 (11.25)	140	510 (10 300), 456 (sh) (6470), 346 (11 450), 294 (56 200), 245 (30 400), 215 (21 300)
2	49.3 (49.45)	3.25 (3.3)	11.65 (11.55)	145	500 (6100), 338 (10 500), 292 (49 500), 245 (26 100), 218 (21 250)

[a] Calculated values are in parentheses. [b] In acetonitrile solution. [c] In acetonitrile solution at 298 K.

80% in each case. Use of the route in Scheme 1 with HL^2 and that in Scheme 2 with HL^1 did not give good results.

The complexes are soluble in both polar and non-polar solvents and slightly in water. Their microanalytical data (Table 1) are in good agreement with the calculated values and thus confirm the composition of the mixed-ligand tris-chelates, $[Ru(bipy)_2L]ClO_4$. The complexes act as 1:1 electrolytes in acetonitrile solution (Table 1). Solid-state magnetic moment measurements at room temperature indicated that the monocations **1** and **2** are diamagnetic (t_{2g}^6, idealised, $S = 0$).

Infrared spectra

The Fourier-transform IR spectra for the complexes were recorded as KBr discs in the range 4000–400 cm^{-1} and display several sharp bands of different intensities. A very strong and broad band near 1100 cm^{-1} and a strong and sharp vibration band near 630 cm^{-1} are observed for both complexes due to the presence of ionic perchlorate. The other expected vibrations due to 2,2′-bipyridine, L^1 and L^2 are systematically present in the spectra and are therefore not specifically reported here.

Electronic spectra

Solution electronic spectra of the complexes were studied in acetonitrile solvent in the UV/VIS region (200–700 nm). Data are listed in Table 1 and spectra are shown in Fig. 1. Multiple absorptions may arise due to the presence of different acceptor levels in the complexes.[3] Complex **1** exhibits one band at 510 nm associated with a shoulder at 456 nm and another band near 350 nm. In the visible region the spectrum of complex **2** is virtually identical to that of **1** except the lowest-energy band does not have an associated shoulder and the bands are slightly blue shifted.

The two visible bands have been assigned on the basis of reported spectra of $[Ru(bipy)_2]^{2+}$ complexes having other kinds of chelating third ligands.[4] With respect to the C_2 axis of the bipyridine ligand, there are two different kinds of bipyridine acceptor orbitals, one symmetric (χ) and one antisymmetric (ψ) and the transitions from metal-filled d_π orbitals to these two π* orbitals result in the above-mentioned bands. Thus these are believed to represent metal-to-ligand charge-transfer (m.l.c.t.) transitions and are expected for low-spin ruthenium(II) complexes. The lower-energy band at ≈500 nm is considered to be due to the $\pi(Ru) \longrightarrow \pi^*(\psi)$ and the higher-energy band near 340 nm to the $d_\pi(Ru) \longrightarrow \pi^*(\chi)$ transition. The bands in the UV region are of intraligand (π–π*) type or charge-transfer transitions involving levels which are higher in energy than those of the ligand lowest unoccupied molecular orbital (LUMO).

The lowest-energy m.l.c.t. band of $[Ru^{II}(bipy)_3]^{2+}$ appears at 450 nm,[5] thus the replacement of one bipy ligand by an asymmetric ligand (L^1 or L^2) results in a red-shift of the same transition. The lower ligand-field strength of L^1 and L^2 compared to bipy and overall lowering of the molecular symmetry on going from $[Ru(bipy)_3]^{2+}$ to complexes **1** and **2** might be possible reasons for the observed shift.

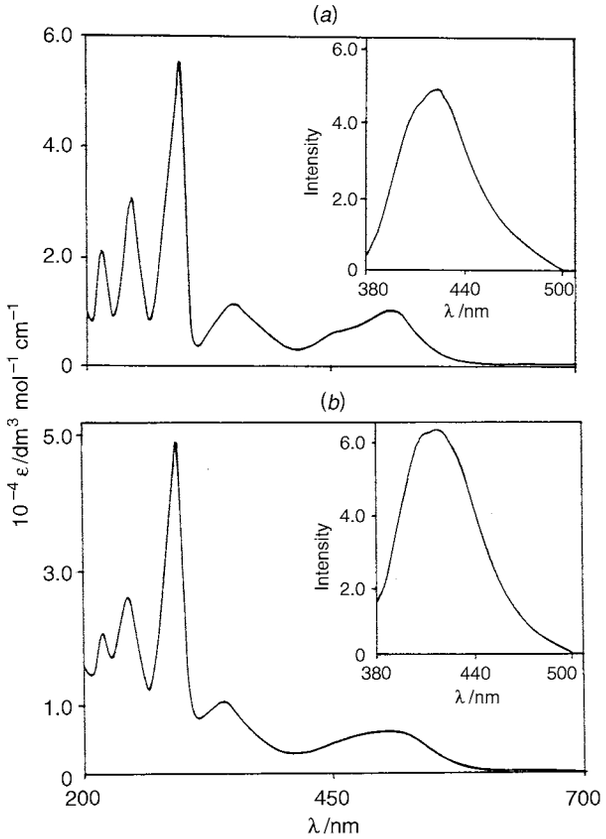

Fig. 1 Electronic spectra of (*a*) $[Ru^{II}(bipy)_2L^1]ClO_4$ **1** and (*b*) $[Ru^{II}(bipy)_2L^2]ClO_4$ **2** in acetonitrile. The insets show the emission spectra at 298 K in acetonitrile

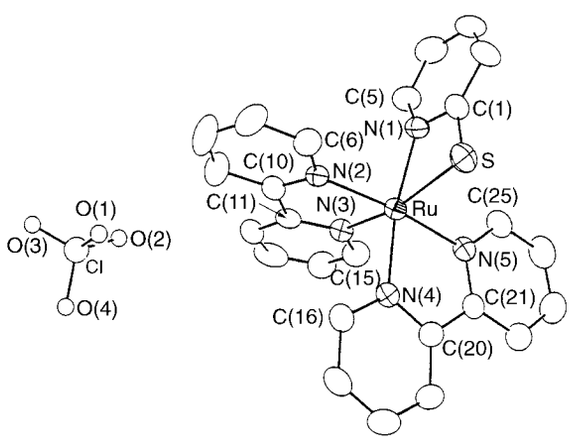

Fig. 2 An ORTEP[6] plot for complex **1**

Crystal structure of $[Ru^{II}(bipy)_2L^1]ClO_4$

The crystal structure of the pyridine-2-thiolato complex **1** is shown in Fig. 2. Selected bond lengths and angles are listed in Table 2. The complex is monomeric and the lattice consists of one type of molecule where the pyridine-2-thiolate ligand is in bidentate mode, co-ordinating through its nitrogen and sulfur atoms. The RuN_5S co-ordination sphere is distorted octahedral as can be seen from the angles subtended at the metal. Distortion from the ideal octahedral geometry is due primarily to the customary N–Ru–N bite angles of the bipyridine ligands (average 78.85°) and N–Ru–S bite angle of the pyridine-2-thiolate

Table 2 Selected bond distances (Å) and angles (°) and their standard deviations for $[Ru(bipy)_2L^1]ClO_4$ **1**

Ru–N(1)	2.060(7)	N(2)–C(10)	1.339(11)
Ru–N(2)	2.058(7)	N(3)–C(11)	1.339(11)
Ru–N(3)	2.044(7)	N(3)–C(15)	1.348(10)
Ru–N(4)	2.036(6)	N(4)–C(16)	1.356(11)
Ru–N(5)	2.042(7)	N(4)–C(20)	1.370(11)
Ru–S	2.434(3)	N(5)–C(21)	1.353(10)
S–C(1)	1.733(9)	N(5)–C(25)	1.357(11)
N(1)–C(5)	1.327(11)	C(20)–C(21)	1.459(12)
N(1)–C(1)	1.372(13)	C(10)–C(11)	1.479(11)
N(2)–C(6)	1.340(10)		
N(1)–Ru–N(2)	90.6(3)	N(1)–Ru–N(3)	99.2(3)
N(1)–Ru–N(4)	170.1(3)	N(1)–Ru–N(5)	94.6(3)
N(2)–Ru–N(3)	78.8(3)	N(2)–Ru–N(4)	96.3(2)
N(2)–Ru–N(5)	173.6(3)	N(3)–Ru–N(4)	89.2(3)
N(3)–Ru–N(5)	96.7(3)	N(4)–Ru–N(5)	78.9(3)
N(1)–Ru–S	68.6(2)	N(2)–Ru–S	97.6(2)
N(3)–Ru–S	167.3(2)	N(4)–Ru–S	103.4(2)
N(5)–Ru–S	87.8(2)	Ru–N(1)–C(1)	102.2(5)
Ru–N(1)–C(5)	136.6(7)	Ru–N(2)–C(6)	126.4(6)
Ru–N(2)–C(10)	115.0(5)	Ru–N(3)–C(11)	116.4(5)
Ru–N(3)–C(15)	126.0(6)	Ru–N(4)–C(16)	126.4(6)
Ru–N(4)–C(20)	116.1(5)	Ru–N(5)–C(21)	115.7(5)
Ru–N(5)–C(25)	126.2(6)	Ru–S–C(1)	79.0(3)
C(1)–N(1)–C(5)	120.9(8)	C(6)–N(2)–C(10)	118.6(7)
C(11)–N(3)–C(15)	117.6(7)	C(16)–N(4)–C(20)	117.5(7)
C(21)–N(5)–C(25)	118.1(7)	N(1)–C(1)–S	109.9(6)

ligand [68.6(2)°]. When ruthenium(II) is bonded to the sulfur atom (thiol) of an organic moiety the average observed Ru^{II}–S bond distance is 2.38 Å.[7] The Ru^{II}–S distance in the present case, 2.434(3) Å, is a bit longer, but compares well with those (2.434 and 2.437 Å) in $[Ru^{II}L^1{}_2(PPh_3)_2]$.[8] The Ru–N (bipy) bond lengths lie in the range 2.036–2.058 Å which fall within the limit of Ru–N (bipy) distances (2.0–2.12 Å) observed earlier.[9] The longest Ru–N distance in the complex is Ru–N(1) (of the pyridine-2-thiolate) 2.060(7) Å. The structural data clearly indicate that in the complex the pyridine-2-thiolate ligand suffers from considerable strain. Thus the Ru–N(1)–C(1) and N(1)–C(1)–S angles [102.2(5) and 109.9(6)° respectively] are reasonably distorted from the 120° expected for sp^2-hybridised atoms. The Ru–S–C(1) angle is 79.0(3)° compared with 90° expected if the sulfur atom bonded using pure p orbitals. Among the angles about ruthenium, N(1)–Ru–S (arising from pyridine-2-thiolate) 68.6(2)° shows the largest deviation from the ideal octahedral co-ordination.

The ClO_4^- anion is tetrahedral with an average Cl–O distance of 1.337 Å and an average O–Cl–O angle of 109.45°.

^{1}H NMR spectra

The NMR spectra of both complexes were recorded in $CDCl_3$ solvent at 300 MHz (Fig. 3).The presence of the asymmetric pyridine-2-thiolate or -2-olate ligand assures non-equivalence of all five pyridine groups. The molecules thus contain 20 non-equivalent aromatic protons each. Since the electronic environments of many pyridine hydrogen atoms are very similar, their signals may appear in a narrow chemical shift range. The spectra of both complexes display twenty signals each of which is clearly observable from the relative intensity of the peaks as expected. Owing to partial overlapping it is difficult to assign all the individual proton signals, however with the aid of a ^{1}H correlation spectroscopy (COSY) experiment the observed 20 signals could be separated into five groups of four, each corresponding to H^3, H^4, H^5 and H^6 of the pyridine ring (usual numbering).

In the complexes the equatorial plane contains two pyridine rings of one bipyridine ligand (c,d), one pyridine ring of the other bipyridine ligand (a) and the sulfur or oxygen atom of the pyridine-2-thiolate or -2-olate ligand. The axial positions are

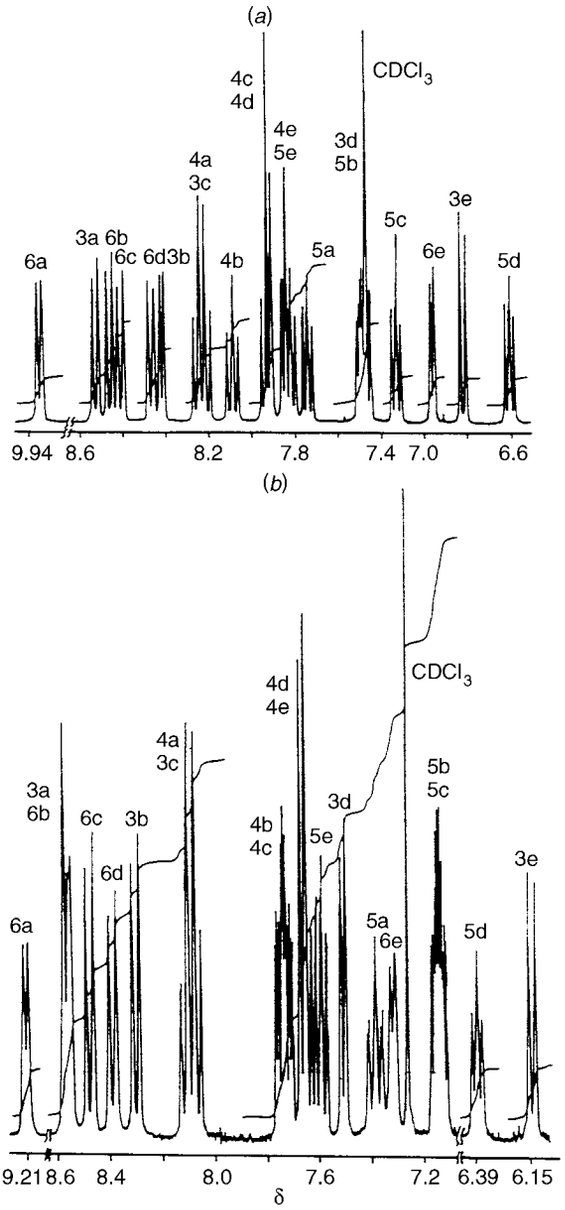

Fig. 3 Proton NMR spectra of (*a*) complex **1** and (*b*) **2** in $CDCl_3$

occupied by the other pyridine ring of the second bipy ligand (b) and the pyridine ring (e) of ligand L. The signals of the equatorial pyridine ring (d) which is *trans* to the σ-donor sulfur or oxygen of L are expected to be different from the other resonances, since they experience the *trans* effect of the thiolato and the phenolato group respectively.

On the basis of the above argument, the signal which appeared at the highest field for the individual H^6, H^5, H^4 and H^3 was assigned to the corresponding 'd'-ring. The H^6 (d) signal of the thiolato complex appears at δ 8.28 while the same signal in the spectrum of the phenolato complex appears at δ 8.38; this implies that the thiolato group has a greater *trans* effect compared to the phenolato group. The order of the pyridine ring protons in increasing field strength is 6 > 3 > 4 > 5 for rings a–c, but for pyridine ring d it is 6 > 4 > 3 > 5. A similar pattern of signals has been observed for other $[Ru(bipy)_2L]$ systems where L is an asymmetric bidentate ligand.[2,9] Except for the pyridine ring (d) proton signals, the other sets cannot be unambiguously assigned to particular pyridyl rings. The substituted-pyridine ring (e) protons follow the order 4 > 5 > 6 > 3 with increasing field strength. The effect of the phenolic oxygen and the thiolato group on the chemical shifts of the proton resonances of pyridine ring e has been observed, *e.g.* H^3 and H^6 for complex **1** (where the thiolato group is pres-

Table 3 Electrochemical data at 298 K [a]

Compound	E°_{298}/V (ΔE_p/mV) Ru^{III}–Ru^{II} couple	Ru^{IV}–Ru^{III} couple	Ligand reduction	ΔE° [b]/V	$\tilde{\nu}_{m.l.c.t.}$/cm^{-1} Obs. [c]	Calc. [d]
1	0.54 (90)	1.41 (130)	−1.63 (70) −1.90 (80)	2.17	19 608	20 501
2	0.64 (100)	1.03 (150)	−1.57 (80) −1.92 (90)	2.21	20 000	20 824

[a] Solvent, acetonitrile; supporting electrolyte, NEt_4ClO_4; reference electrode, SCE; solute concentration, 10^{-3} mol dm^{-3}; working electrode, platinum wire. Cyclic voltammetric data: scan rate, 50 mV s^{-1}; $E^{\circ}_{298} = 0.5(E_{pc} + E_{pa})$ where E_{pc} and E_{pa} are cathodic and anodic peak potentials respectively. [b] Calculated by using equation (5) of text. [c] In acetonitrile solution. [d] Using equation (4) of text.

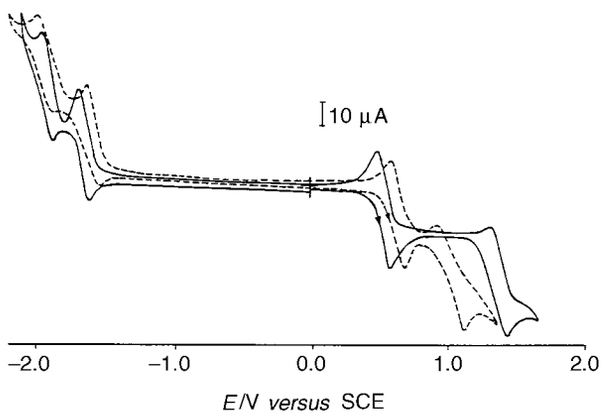

Fig. 4 Cyclic voltammograms of ≈10^{-3} mol dm^{-3} solutions of complexes **1** (——) and **2** (– – –) in acetonitrile at 298 K

ent) appear at δ 6.81 and 6.88 respectively, whereas for **2** (where a phenolato group is present) they appear at δ 6.15 and 7.33.

Electron-transfer properties

The electron-transfer properties of both complexes have been studied by cyclic voltammetry in acetonitrile solvent (supporting electrolyte, 0.1 mol dm^{-3} NEt_4ClO_4; working electrode, platinum). All the potentials are referenced to the saturated calomel electrode (SCE). Both complexes are electroactive with respect to the metal as well as the ligand centres and display the same four redox processes in the potential range ±2 V at 298 K. Voltammograms are shown in Fig. 4, reduction potentials in Table 3. The assignment of the responses to specific couples are based on the following considerations.

Ruthenium(III)–ruthenium(II) couple. Complexes **1** and **2** exhibit one quasi-reversible oxidative response with E°_{298} values of 0.54 and 0.64 V respectively. The anodic and cathodic peak heights are approximately equal and vary with the square root of the scan rate. The peak potentials E_{pa} and E_{pc} are virtually independent of the scan rate. This quasi-reversible oxidative process is assigned to the ruthenium(III)–ruthenium(II) couple, equation (1). The one-electron nature of this process for both

$$[Ru^{III}(bipy)_2L]^{2+} + e^- \rightleftharpoons [Ru^{II}(bipy)_2L]^+ \qquad (1)$$

complexes was confirmed by constant-potential coulometry (see Experimental section). The complexes are unstable to oxidation at room temperature. The formal potential of the couple varies depending on the donor sites present in the ligand. The complexes have an identical RuN_5 core but the sixth co-ordination site in one case is a thiolato group and in the other it is a phenolato group. The effect of the different sixth donor is clearly reflected in the metal redox potential. The 100 mV positive shift on going from the thiolate to phenolate ligand implies that the stability of the bivalent ruthenium in the phenolato environment is greater. The electronegativity difference between the oxygen and sulfur centres may account for the observed trend in redox stability.

Under identical experimental conditions, the ruthenium(III)–ruthenium(II) couple of $[Ru(bipy)_3]^{2+}$ appears at 1.29 V.[3,5] Thus substitutions of one bipy ligand, which is a well known π-acidic ligand, by σ-donating thiolate (L^1) and phenolate (L^2) ligands result in a decrease in potential by 0.75 and 0.65 V respectively. The monoanionic thiolate (L^1) and phenolate (L^2) ligands reduce the overall charge of the complex cation from +2 in $[Ru(bipy)_3]^{2+}$ to +1 in the present complexes. This reduction provides further electrostatic stabilisation of the oxidised species, *i.e.* trivalent $Ru^{III}L$. This decrease of metal oxidation potential and the reversible nature of the voltammograms (Fig. 4) indicate the possibility of generating trivalent congeners of **1** and **2** with the present mixed-ligand environments.

Although the redox potentials for both complexes are not too high, the complexes are unstable upon electrochemical as well as chemical oxidation at room temperature. The presence of the four-membered chelating ring in the complexes causes some strain in the molecule and this might be one of the contributing factors to the instability.

The complexes display a second quasi-reversible oxidation above 1 V. For the thiolato complex **1** it appears near 1.41 V and for the phenolato complex near 1.03 V. The one-electron nature of this oxidation process for both complexes is confirmed by direct comparison of the current height of these second processes with those of the previous one-electron ruthenium(III)–ruthenium(II) reduction process. The second oxidation process could be due to either ruthenium(III) ⟶ ruthenium(IV) oxidation or oxidation of the co-ordinated thiolato and phenolato groups. Since both the free HL^1 and HL^2 (protonated or as deprotonated sodium salts) do not show any electrooxidation within the specified potential range and the order of the second oxidation potentials for the complexes (**1** > **2**) is consistent with sulfur-donor atom stabilisation of the lower oxidation states of the metal ion, we believe that this second oxidation may be due to Ru^{III}–Ru^{IV} oxidation. Constant-potential coulometry failed to generate the second oxidised species precluding the further detailed characterisation. The potential differences between the two successive oxidation processes for the thiolato (**1**) and phenolato (**2**) complexes are 0.8 and 0.3 V respectively. These values are much lower than previously observed average potential difference, 1.3–1.5 V, for the two successive redox processes of the ruthenium centre [(Ru^{II}–Ru^{III}) − (Ru^{III}–Ru^{IV})] in mononuclear complexes.[9,10] The presence of the strongly sterically compressed chelate-ring system (pyridine-2-thiolato or -2-olato) may account for the observed behaviour.

Ligand reduction. Both complexes display two successive reversible one-electron reductions near −1.6 and −1.9 V (Fig. 4, Table 3). The ligand L does not exhibit any ligand reduction within the above-mentioned potential region. Thus the above reductions are assigned to the co-ordinated bipy ligands. It is well established that bipy is a potential electron-transfer centre.

Each bipy can accept two electrons in one electrochemically accessible lowest unoccupied molecular orbital (LUMO).[11,12] Reductions of bipy involve the diimine (−N=C−C=N−) fragment. Complexes **1** and **2** contain two bipy ligands so that four successive reductions are expected from each. In practice two one-electron reductions have been observed for each complex, which are assigned to the diimine groups of the co-ordinated bipy ligands as shown in equations (2) and (3). The other two reductions are not detected presumably due to solvent cut-off.

$$[Ru(bipy)_2L]^+ + e^- \rightleftharpoons [Ru(bipy)(bipy^{\bullet -})L] \quad (2)$$

$$[Ru(bipy)(bipy^{\bullet -})L] + e^- \rightleftharpoons [Ru(bipy^{\bullet -})_2L]^- \quad (3)$$

Spectroelectrochemical correlation

Complexes **1** and **2** display lowest m.l.c.t. transitions of the type $t_2(Ru) \longrightarrow$ ligand LUMO (where the LUMO is dominated by the diimine function of the bipy ligand) at 510 and 500 nm respectively (Table 1). The quasi-reversible ruthenium(III)–ruthenium(II) reduction potentials are 0.54 and 0.64 V, and the first ligand reductions at −1.63 and −1.57 V respectively. Here the m.l.c.t. transition involves excitation of the electron from the filled t_{2g}^6 orbital of ruthenium(II) to the lowest π* orbital of the diimine function. The energy of this band can be predicted from the experimentally observed electrochemical data with the help of equations (4) and (5).[13] Here $E^\circ_{298}(Ru^{III}–Ru^{II})$ is the

$$\nu_{m.l.c.t.} = 8065(\Delta E^\circ) + 3000 \quad (4)$$

$$\Delta E^\circ = E^\circ_{298}(Ru^{III}–Ru^{II}) - E^\circ_{298}(L) \quad (5)$$

formal potential (in V) of the quasi-reversible ruthenium(III)–ruthenium(II) couple, $E^\circ_{298}(L)$ that of the first ligand reduction and $\nu_{m.l.c.t.}$ is the frequency or energy of the charge-transfer band in cm^{-1}. The factor 8065 is used to convert the potential difference ΔE from V into cm^{-1} unit and the term 3000 cm^{-1} is of empirical origin. The calculated and experimentally observed $\nu_{m.l.c.t.}$ transitions are listed in Table 3. Here the calculated values for both complexes lie within 900 cm^{-1} of the experimentally observed charge-transfer energies, which are in good agreement with the observations of previous workers on other mixed-ligand bipy[14] and azopyridine systems.[13]

Room-temperature emission spectra

Excitation of the thiolato complex **1** at 510 nm in acetonitrile solution at room temperature resulted in very weak emission near 600 nm, however excitation at 346 nm gave a moderately strong emission at 420 nm [Fig. 1(*a*)]. The origin of the latter emission was further confirmed by the excitation spectrum of the same solution. Similarly, at room temperature the phenolato complex **2** when excited at 500 nm exhibits very weak emission near 600 nm, but excitation at 338 nm results in moderately strong emission at 416 nm [Fig. 1(*b*); origin confirmed by the excitation spectrum]. The lifetime of the excited states of the thiolato and phenolato complexes are found to be 100 and 90 ns respectively, at room temperature.

Since both free HL^1 and HL^2 and their sodium salts exhibit emission around 400 nm at room temperature, the observed emissions for complexes **1** and **2** near 400 nm probably originate from the co-ordinated pyridine-derived L^1 and L^2.

Electrogeneration of trivalent ruthenium congener, and distortion parameters

At room temperature the electrogenerated trivalent analogues of complexes **1** and **2** are unstable both in dichloromethane and acetonitrile solvents, decomposing to unidentifiable products. However, at 263 K coulometric oxidations of **1** and **2** in dichloromethane at 0.6 and 0.7 V *vs.* SCE respectively generate tractable oxidised greenish solutions (observed Coulomb count corresponds to one-electron transfer; *n* for **1** and **2** are 1.08 and 1.05 respectively where $n = Q/Q'$, Q is the calculated Coulomb count for a one-electron transfer and Q' that found after exhaustive electrolysis of a 10^{-2} mmol solution of the complex).

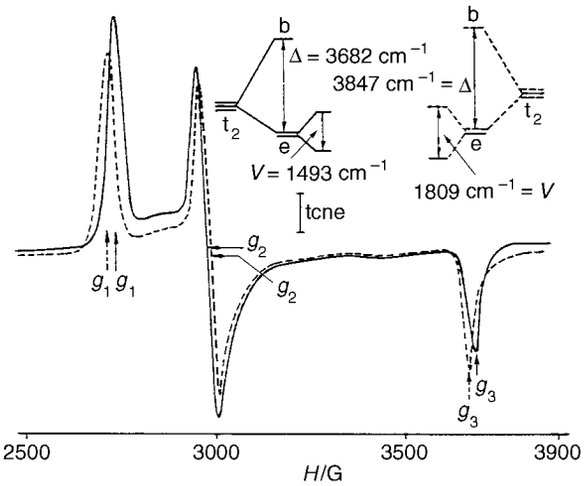

Fig. 5 X-Band EPR spectra and t_2 splittings of the coulometrically oxidised complexes **1** (——) and **2** (– – –) in dichloromethane solution at 77 K

In order to confirm that the oxidised solutions contain oxidised metal (trivalent ruthenium) as opposed to oxidised ligand, the X-band EPR spectra of fresh solutions (produced coulometrically at 263 K followed by quick freezing in liquid N_2, 77 K) of species $\mathbf{1}^+$ and $\mathbf{2}^+$ were examined (Fig. 5). The rhombic spectra are characteristic of low-spin trivalent ruthenium complexes (low spin, t_{2g}^5, $S = \frac{1}{2}$) in a distorted-octahedral environment.[15] The starting bivalent mixed-ligand tris-chelates **1** and **2** have distorted-octahedral geometry in the vicinity of the ruthenium ion. Rhombic EPR spectra are therefore expected for both the oxidised trivalent ruthenium species, $\mathbf{1}^+$ and $\mathbf{2}^+$.

The theory of the EPR spectra of distorted-octahedral low-spin d^5 (idealised t_{2g}^5, ground term $^2T_{2g}$) complexes is documented.[15,16] The distortion can be expressed as a sum of axial (Δ) and rhombic (*V*) components. The t_2 orbital consists of the components t_2^0 (*xy*), t_2^+ (*xz*) and t_2^- (*yz*).[16] The degeneracy of the t_2 orbital is partly removed by axial distortion (Δ), which places t_2^0 (b) above t_2^+/t_2^- (e). The superimposed rhombic distortion then splits (e) further into t_2^+ and t_2^-. The analysis of the EPR spectra using the *g*-tensor theory of low-spin d^5 ions provides the distortion parameters (Δ and *V*) of the complexes and the energies of two crystal-field transitions (ν_1 and ν_2) which arise due to optical transitions from ground to upper Kramers doublets.[15]

The EPR experiments give only the absolute *g* values and so neither their signs nor the correspondence of g_1, g_2 or g_3 to g_x, g_y or g_z are known. There are forty eight possible combinations based on the labelling (*x*,*y*,*z*) and signs chosen for the experimentally observed *g* values. In the present cases we have taken the combination where g_1 and g_2 are negative, g_3 is positive and the order of magnitude is $g_1 > g_2 > g_3$ as only this gives the reasonable value of k (<1.0). The value of k for all other combinations of *g* parameters does not fall within the limit $k < 1.0$. The orbital reduction factor (k), axial distortion (Δ/λ), rhombic distortion (V/λ) and the two ligand-field transitions (ν_1/λ and ν_2/λ) for both the complexes are listed in Table 4. The value of the spin–orbit coupling constant (λ) of ruthenium(III) is taken as 1000 cm^{-1}.[15] In the case of the thiolato complex $\mathbf{1}^+$ the axial distortion is approximately 2.5 times more than the rhombic distortion, whereas the phenolato complex $\mathbf{2}^+$ exhibits 2 times more axial distortion than rhombic distortion.

Experimental

Materials

Commercial ruthenium trichloride (S.D. Fine chemicals, Bombay, India) was converted into $RuCl_3 \cdot 3H_2O$ by repeated evaporation to dryness with concentrated hydrochloric acid. The complexes *cis*-$[Ru(bipy)_2Cl_2] \cdot 2H_2O$ and *cis*-$[Ru(bipy)_2(CO_3)]$ were prepared according to the reported procedure.[17,18] Pyridine-2-thiol and pyridin-2-ol were obtained from Aldrich, USA. Other chemicals and solvents were reagent grade and used as received. Silica gel (60–120 mesh) for chromatography was of BDH quality. For spectroscopic/electrochemical studies HPLC grade solvents were used. Commercial tetraethylammonium bromide was converted into pure tetraethylammonium perchlorate by following an available procedure.[19] Dinitrogen gas was purified by successively bubbling it through alkaline dithionite and concentrated sulfuric acid.

Physical measurements

Solution electrical conductivity was checked using a Systronic 305 conductivity bridge. Electronic spectra (700–200 nm) were recorded using a Shimadzu-UV-265 spectrophotometer, Fourier-transform IR spectra on a Nicolet spectrophotometer with samples prepared as KBr pellets. Magnetic susceptibility was checked with a PAR vibrating-sample magnetometer. Proton NMR spectra were obtained with a 300 MHz Varian Fourier-transform spectrometer. Cyclic voltammetric measurements were carried out using a PAR model 362 scanning-potentiostat electrochemistry system. Platinum-wire working and auxiliary electrodes and an aqueous saturated calomel reference electrode (SCE) were used in a three-electrode configuration. The supporting electrolyte was NEt_4ClO_4 and the solute concentration was $\approx 10^{-3}$ mol dm^{-3}. The half-wave potential E°_{298} was set equal to $0.5(E_{pa} + E_{pc})$, where E_{pa} and E_{pc} are the anodic and cathodic cyclic voltammetric peak potentials respectively. The scan rate was 50 mV s^{-1}. The coulometric experiments were done with a PAR model 370-4 electrochemistry apparatus incorporating a 179 digital coulometer. A platinum wire-gauze working electrode was used. All experiments were carried out under a dinitrogen atmosphere and are uncorrected for junction potentials. The EPR measurements were made with a Varian model 109C E-line X-band spectrometer fitted with a quartz dewar for measurements at 77 K (liquid nitrogen). The spectra was calibrated by using tetracyanoethylene (tcne) ($g = 2.0037$). The elemental analyses were carried out with a Carlo Erba (Italy) elemental analyser. Solution emission properties were checked using a SPEX-fluorolog spectrofluorometer.

CAUTION: perchlorate salts of metal complexes are generally explosive and care should be taken while handling them.

Preparation of complexes

Bis(2,2′-bipyridine)(pyridine-2-thiolato)ruthenium(II) perchlorate 1. The complex $[Ru(bipy)_2Cl_2] \cdot 2H_2O$ (100 mg, 0.19 mmol) and $AgClO_4$ (80 mg, 0.39 mmol) were taken in dry ethanol (30 cm^3) and the mixture was heated to reflux with stirring. The initial violet solution changed to orange-red. It was then cooled and filtered through a Gooch sintered-glass funnel. The filtrate (ethanolato species) was taken in a three-necked flask and flushed with nitrogen gas for 15 min. To this were added pyridine-2-thiol HL^1 (32 mg, 0.29 mmol) and anhydrous sodium acetate (24 mg, 0.29 mmol). The whole mixture was stirred magnetically under nitrogen overnight. The precipitate thus formed was filtered off and washed thoroughly with ice-cold distilled water and then with diethyl ether. The crystalline solid mass was dried *in vacuo* over P_4O_{10}. It was dissolved in a small volume of chloroform and subjected to chromatography on a silica gel (60–120 mesh) column. A brick-red band was eluted with acetonitrile–chloroform (1 : 2). This fraction was collected and evaporated under reduced pressure to yield crystalline $[Ru(bipy)_2L^1]ClO_4$, yield 96 mg (80%).

Bis(2,2′-bipyridine)(pyridin-2-olato)ruthenium(II) perchlorate 2. The complex $[Ru(bipy)_2(CO_3)]$ (100 mg, 0.21 mmol) was dissolved in dry ethanol (25 cm^3). Pyridin-2-ol (40 mg, 0.42 mmol) and anhydrous sodium acetate (35 mg, 0.42 mmol) were added. The resulting mixture was heated to reflux with stirring for 3 h. The initial violet solution gradually turned red. The progress of the reaction was monitored periodically by TLC. The volume of the solvent was then reduced under reduced pressure and a saturated aqueous solution (5 cm^3) of $NaClO_4$ was added. The dark precipitate thus obtained was filtered off and washed with ice-cold water and then with diethyl ether. The solid mass was dried *in vacuo* over P_4O_{10}. The product $[Ru(bipy)_2L^2]ClO_4$ was pure. Yield 115 mg (90%).

Crystallography

Single crystals of complex **1** were grown by slow diffusion of an acetonitrile solution of it in benzene. A dark crystal of dimensions 0.2 × 0.4 × 0.5 mm was mounted on a glass fibre. Unit-cell parameters were determined by the least-squares fit of 25 machine-centred reflections having 2θ values in the range 15–30°. Lattice dimensions and the Laue group were checked by axial photography. Systematic absences led to the identification of the space group as $P2_1/n$. Data were collected by the ω-scan method over the range 2θ 3–40° ($\pm h, +k, +l$) on a Siemens R3m/V diffractometer with graphite-monochromated Mo-Kα radiation ($\lambda = 0.710\ 73$ Å) at 295 K. Significant crystal data and data collection parameters are listed in Table 5. Two check reflections were measured after every 198 during data collection to monitor crystal stability. No significant intensity reduction was observed during the exposure to X-ray radiation. All data were corrected for Lorentz-polarisation effects. An absorption correction was not applied because of the small absorption coefficient ($\mu = 8.55$ cm^{-1}). Of the 2709 reflections collected 2354

Table 4 The EPR g values[a] and distortion parameters[b]

	Compound	
	1	**2**
g_1	−2.360	−2.378
g_2	−2.172	−2.163
g_3	1.755	1.767
k	0.6086	0.6265
Δ/λ	3.682	3.8465
V/λ	−1.493	−1.808
ν_1/λ	3.0699	3.087
ν_2/λ	4.7619	5.0577

[a] In dichloromethane solution at 263 K. [b] Meanings are given in the text.

Table 5 Crystallographic data for complex **1**

Formula	$C_{25}H_{20}ClN_5O_4RuS$
M	622.6
Crystal symmetry	Monoclinic
Space group	$P2_1/n$
a/Å	10.291(10)
b/Å	13.819(8)
c/Å	18.364(13)
β/°	105.21(7)
U/Å^3	2517(3)
Z	4
D_c/g cm^{-3}	1.644
R[a]	0.053
R'[b]	0.067

[a] $R = \Sigma||F_o| - |F_c||/\Sigma|F_o|$. [b] $R' = [\Sigma w(|F_o| - |F_c|)^2/w|F_o|^2]^{\frac{1}{2}}$, $w^{-1} = \sigma^2(|F_o|) + 0.0005|F_o|^2$.

were unique and 1972 with $F > 6.0\sigma(F)$ were used for structure solution.

All calculations for data reduction, structure solution and refinement were done on a Micro Vax II computer using the SHELXTL PLUS program package.[20] The metal atom was located from a Patterson map and the other non-hydrogen atoms emerged from the Fourier-difference syntheses. The structure was then refined (based on F) by full-matrix least-squares procedures. All non-hydrogen atoms except those belonging to the anion were refined anisotropically. Hydrogen atoms were added at calculated positions with fixed $U = 0.08$ Å^2 in the last cycle of refinement. The number of variable parameters was 314, affording a data-to-parameter ratio of 6.3:1. The refinement converged to $R = 0.053$, $R' = 0.067$ and goodness of fit = 1.09, with the largest difference peak of 1.12 e Å^{-3} near the metal atom.

Atomic coordinates, thermal parameters, and bond lengths and angles have been deposited at the Cambridge Crystallographic Data Centre (CCDC). See Instructions for Authors, *J. Chem. Soc.*, *Dalton Trans.*, 1997, Issue 1. Any request to the CCDC for this material should quote the full literature citation and the reference number 186/425.

Acknowledgements

Financial support received from the Department of Science and Technology, New Delhi, India, is gratefully acknowledged. Crystallography was done at the National Single Crystal Diffractometer Facility, Department of Inorganic Chemistry, Indian Association for the Cultivation of Science, Calcutta, India. We are grateful to Professor A. Q. Contractor and Ms. S. Sukeerthi, Indian Institute of Technology (ITT), Bombay, for assistance with electrochemical measurements and Dr. D. Chatterjee, Central Salt and Marine Chemicals Research Institute, Bhavnagar, India for emission study. Special acknowledgement is made to Regional Sophisticated Instrumentation Centre, IIT Bombay for providing the NMR facility. The comments of the reviewers at the revision stage were very helpful.

References

1 B. J. Coe, D. A. Friesen, D. W. Thompson and T. J. Meyer, *Inorg. Chem*., 1996, **35**, 4575; M. Milkevitch, E. Brauns and K. J. Brewer, *Inorg. Chem.*, 1996, **35**, 1737; C. B. Brennan, P. Subramanian, M. Abasi, C. Stern and J. T. Hupp, *Inorg. Chem*., 1996, **35**, 3719; M. D. Ward, *Inorg. Chem.*, 1996, **35**, 1712; S. C. Rasmussen, D. W. Thompson, V. Singh and J. D. Petersen, *Inorg. Chem.*, 1996, **35**, 3449; J. Bolger, A. Gourdon, E. Ishow and J. P. Launay, *Inorg. Chem*., 1996, **35**, 2937; G. Tresoldi, S. L. Schiavo, P. Piraino and P. Zanello, *J. Chem. Soc., Dalton Trans.*, 1996, 885; A. M. W. Cargill Thompson, J. C. Jeffery, D. J. Liard and M. D. Ward, *J. Chem. Soc., Dalton Trans.*, 1996, 879; M. D. Johnson and D. Nickerson, *Inorg. Chem*., 1992, **31**, 3971; M. A. Greaney, C. L. Coyle, A. J. Harmer and E. I. Stiefel, *Inorg. Chem*., 1989, **28**, 912; M. J. Root and E. Deutsh, *Inorg. Chem*., 1984, **23**, 622; R. Kroener, M. J. Heeg and E. Deutsh, *Inorg. Chem*., 1988, **27**, 558; K. Tanaka, M. Morimoto and T. Tanaka, *Inorg. Chim. Acta*, 1981, **56**, L61; S. Sinha, P. K. Das and B. K. Ghosh, *Polyhedron*, 1994, **13**, 2665; G. A. Thakur, K. Narayanaswamy and G. K. Lahiri, *Indian J. Chem., Sect. A*, 1996, **35**, 379; R. N. Mukherjee and A. Chakravorty, *J. Chem. Soc., Dalton Trans.*, 1983, 2197; M. J. Root, B. P. Sullivan, T. J. Meyer and E. Deutsch, *Inorg. Chem.*, 1984, **24**, 2731; P. Reveco, R. H. Schmehl, W. R. Cherry, F. R. Fronczek and J. Selbin, *Inorg. Chem.*, 1985, **24**, 4078.

2 S. L. Meeklenburg, B. M. Peek, J. R. Schoonover, D. G. McCafferty, C. G. Wall, B. W. Erickson and T. J. Meyer, *J. Am. Chem. Soc.*, 1993, **115**, 5479; R. Alsfasser and R. V. Eldik, *Inorg. Chem*., 1996, **35**, 628; M. Maestri, N. Armaroli, V. Balzani, E. C. Constable and A. M. W. C. Thompson, *Inorg. Chem.*, 1995, **34**, 2759; D. M. Klassen and G. A. Crosby, *J. Chem. Phys.*, 1968, **48**, 1853; P. Chen, R. Deusing, D. K. Graff and T. J. Meyer, *J. Phys. Chem*., 1991, **95**, 5850; B. Noble and R. D. Reacock, *Inorg. Chem*., 1996, **35**, 1616.

3 A. Juris, V. Balzani, F. Barigelletti, S. Campagna, P. Belser and A. V. Zelewsky, *Coord. Chem. Rev.*, 1988, **84**, 85.

4 B. J. Coe, T. J. Meyer and P. S. White, *Inorg. Chem*., 1995, **34**, 593; A. Ceulemansm and L. G. Vanquickenborne, *J. Am. Chem. Soc.*, 1981, **103**, 2238.

5 G. M. Brown, T. R. Weaver, F. R. Keene and T. J. Meyer, *Inorg. Chem*., 1976, **15**, 190.

6 C. K. Johnson, ORTEP, Report ORNL-5138, Oak Ridge National Laboratory, Oak Ridge, TN, 1976.

7 B. K. Santra, G. A. Thakur, P. Ghosh, A. Pramanik and G. K. Lahiri, *Inorg. Chem*., 1996, **35**, 3050; M. M. Millar, T. O'Sullivan, N. DeVries and S. A. Koch, *J. Am. Chem. Soc.*, 1985, **107**, 3714; D. Coucouvanis, *Prog. Inorg. Chem.*, 1979, **26**, 301; S. P. Satsangee, J. H. Hain, P. T. Copper and S. A. Koch, *Inorg. Chem.*, 1992, **31**, 5160; P. J. Blower and J. R. Dilworth, *Coord. Chem. Rev.*, 1987, **76**, 121.

8 S. R. Fletcher and A. C. Skapski, *J. Chem. Soc., Dalton Trans.*, 1972, 635.

9 B. M. Holligan, J. C. Jeffery, M. K. Norgett, E. Schatz and M. D. Ward, *J. Chem. Soc., Dalton Trans.*, 1992, 3345; D. P. Rillema, D. S. Jones and H. A. Levy, *J. Chem. Soc., Chem. Commun.*, 1979, 849.

10 G. K. Lahiri, S. Bhattacharya, B. K. Ghosh and A. Chakravorty, *Inorg. Chem*., 1987, **26**, 4324; N. Bag, G. K. Lahiri, S. Bhattacharya, L. R. Falvello and A. Chakravorty, *Inorg. Chem*., 1988, **27**, 4396; P. Ghosh, A. Pramanik, N. Bag, G. K. Lahiri and A. Chakravorty, *J. Organomet. Chem*., 1993, **454**, 273; G. K. Lahiri, S. Bhattacharya, M. Mukherjee, A. K. Mukherjee and A. Chakravorty, *Inorg. Chem*., 1987, **26**, 3359; S. Chattopadhyay, N. Bag, P. Basu, G. K. Lahiri and A. Chakravorty, *J. Chem. Soc., Dalton Trans.*, 1990, 3389.

11 S. Bhattacharya, *Polyhedron*, 1993, **12**, 235.

12 C. M. Elliott, *J. Chem. Soc., Chem. Commun.*, 1980, 261; N. E. Tokel-Takvoryan, R. E. Hemingway and A. J. Bard, *J. Am. Chem. Soc.*, 1973, **95**, 6582; D. E. Morris, K. W. Hanck and M. K. DeArmond, *Inorg. Chem*., 1985, **24**, 977.

13 S. Goswami, R. N. Mukherjee and A. Chakravorty, *Inorg. Chem*., 1983, **22**, 2825.

14 B. K. Ghosh and A. Chakravorty, *Coord. Chem. Rev.*, 1989, **95**, 239.

15 G. K. Lahiri, S. Bhattacharya, S. Goswami and A. Chakravorty, *J. Chem. Soc., Dalton Trans.*, 1990, 561; P. S. Rao, G. A. Thakur and G. K. Lahiri, *Indian J. Chem., Sect. A*, 1996, **35**, 946; A. Pramanik, N. Bag, G. K. Lahiri and A. Chakravorty, *J. Chem. Soc., Dalton Trans.*, 1990, 3823.

16 B. Bleaney and M. C. M. O'Brien, *Proc. Phys. Soc. London, Sect. B*, 1956, **69**, 1216; J. S. Griffith, *The Theory of Transition Metal Ions*, Cambridge University Press, London, 1961, p. 364; S. Bhattacharya and A. Chakravorty, *Proc. Indian Acad. Sci., Chem. Sci.*, 1985, **95**, 159; R. E. Desimone, *J. Am. Chem. Soc.*, 1973, **95**, 6238; N. J. Hill, *J. Chem. Soc., Faraday Trans.*, 1972, 427; C. J. Ballhausen, *Introduction to Ligand Field Theory*, McGraw-Hill, New York, 1962, p. 99.

17 B. P. Sullivan, D. J. Salmon and T. J. Meyer, *Inorg. Chem*., 1978, **17**, 3334.

18 E. C. Johnson, B. P. Sullivan, D. J. Salmon, S. A. Adeyemi and T. J. Meyer, *Inorg. Chem*., 1978, **17**, 2211.

19 D. T. Sawyer and J. L. Roberts, jun., *Experimental Electrochemistry for Chemists*, Wiley, New York, 1974, p. 167.

20 G. M. Sheldrick, SHELXTL PLUS, Structure Determination Software Program, Siemens Analytical X-Ray Instruments Inc., Madison, WI, 1990.

Received 7*th October* 1996; *Paper* 6/06871E